



Phase-Field Modeling of Electrochemical Phenomena

Saswata Bhattacharyya^{1*}, Soumya Bandyopadhyay^{1†} and Abhik Choudhury^{2‡}

Abstract | In this article, we review the progress in the field of application of phase-field models for simulating electrochemical phenomena such as etching, electro-deposition, electromigration, intercalation etc. As we will see the present models can be considered as extensions of the already existing models for diffusion coupled phase transformations. We briefly visit the essential thermodynamics of the electrochemical interfaces and the basis of phase-field formulations existing in literature for modeling electrochemical reactions and electromigration. Thereafter, we give a brief overview of the present state of literature in this field.

1 Introduction

Phase-field modeling has been used extensively in investigations of phase transformations and pattern formations in many areas such as solidification, solid-state transformations, and other elastic and magneto-elastic coupled problems.¹⁻³ In this paper, we discuss the developments in the field of phase-field modeling for simulations electrochemistry of related applications.

In literature, there are a number of models written down for the application to problems involving electrochemical reactions. Guyer et al.^{4,5} discuss a general description for the including electromigration in the phase-field equations of the Allen-Cahn type, however, coupling of electrochemical reactions whose rates are described by the Butler-Volmer type equations are not explicitly discussed. Subsequent efforts⁶ have extended the model to include electrochemical-hydrodynamic interactions in nano-channels. A general feature of the model requires the discretization of the double layer where there are rapid changes in the composition and the charge density, requiring fine discretization. This has led to model simplifications as described by Shibuta et al.^{7,8} and others,⁹ who extend the KKS type¹⁰ model for solidification to electrochemical reactions. However the authors circumvent computational problem of the treatment of double

layers through a simplification of imposing charge neutrality which is valid when time-scale of charge re-distribution is much smaller as compared that to the relaxation of the long-range diffusion field. Thus, the authors apply the model to instabilities at the growth front leading to dendrites, which are mass-diffusion controlled and the potential distribution follows from the continuity of the current. This simplification is, however, valid only for certain applications such as in electrolysis of molten-salts and has been applied to these applications by different authors,^{11,12} who extend a Cahn-Hilliard model for incorporating chemical reactions. The other extreme of reaction-controlled evolution such as spinodal decomposition during intercalation has been investigated by,¹³⁻¹⁶ where again the structure and influence of the dynamics of the electrochemical interface is ignored. The current is related to the over-potential through the generalized Butler-Volmer type equation, and the current exchange density J_o , which is a pre-factor of the Butler-Volmer equation is a function of the composition and the compositional gradients. The general frame-work of including the reaction into the mass conservation equation in the general phase-field models solving the entire set of Poisson-Nernst-Planck equations (PNP),^{4,5,13} is discussed separately^{13,17} in a manner that is similar in treatment to what has been stated in a mean-field lattice gas model.¹⁸

¹Department of Materials Science and Metallurgical Engineering, Indian Institute of Technology, Hyderabad, India.

²Department of Materials Engineering, Indian Institute of Science, 560012 Bangalore, India.

*saswata@iith.c.in

†ms13m14p100001@iith.ac.in

‡abhiknc@materials.iisc.ernet.in

2 The Equilibrium Electrochemical Interface

In this section, we discuss certain properties about the electrochemical equilibrium between two phases α , β . For this, we develop the thermodynamic discussion from the case of pure materials to binary alloys and thereafter an electrochemical interface.

2.1 Pure material

Let us start from the equilibrium of a pure material, i.e. consisting of a single element which exhibits a phase transformation (say melting) from α (solid) to β (liquid) above a temperature T_m (melting point). At the equilibrium temperature T_m , the phases α and β co-exist and at this temperature the **driving force** of phase transformation, which is the difference of the free-energies between the phases is zero, $f_\alpha(T_m) = f_\beta(T_m)$, where f_α and f_β are the free energy densities of the α and β phases respectively. The situation can be depicted using the following schematic Fig. 1, where above T_m the free-energy of α (solid) is greater than that of the β (liquid), which implies a driving force for

melting and conversely for $T < T_m$, where there is driving force for solidification. At the equilibrium temperature T_m , the internal energies of both phases can be shown to have a jump, at the interface between the phases α and β following the release of latent heat at the interface which is the difference of the internal energies of the solid and the liquid phases.

2.2 Alloys

Now, let us visit the case of alloys, and for simplicity consider a binary alloy. At a given temperature the free-energy of each of the phases can be described as functions of compositions. Equilibrium between the two phases then is described using the well known common tangent construction, which gives the compositions of the phases in equilibrium as well as the region of compositions at a given temperature where a two-phase existence can be expected. The situation of equilibrium can be visualized through the following schematic Fig. 2. The common tangent construction can be visualized equivalently by performing a Legendre transform of the free-energy density (see Fig. 3),

Driving force: Difference between the grand-potential densities of the phases which reduces to the difference of the free-energy densities for the case of the pure materials.

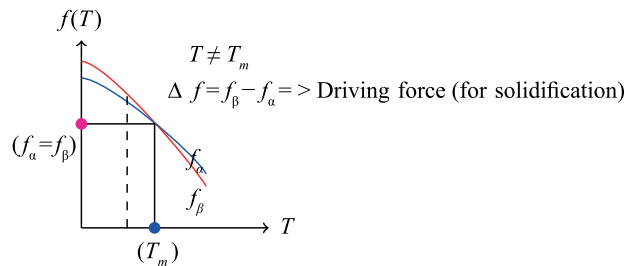


Figure 1: Schematic of the variation of free energies of the α (solid) and the β (liquid) with temperature. At $T = T_m$, the free-energies of both the phases are equal.

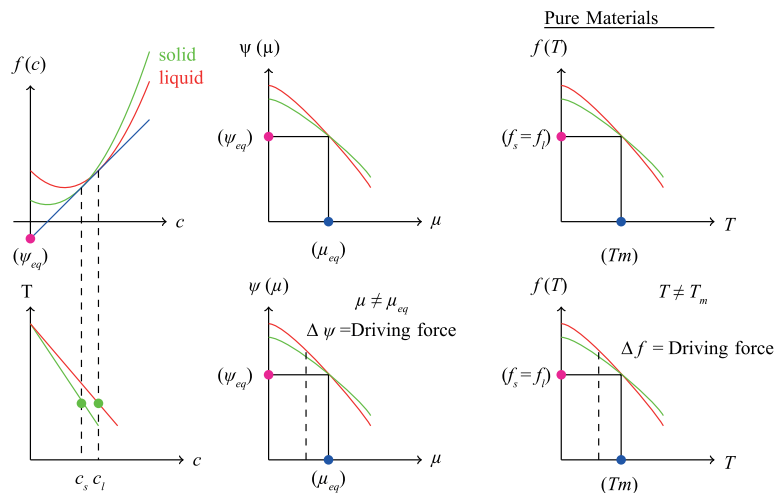


Figure 2: Equilibrium in a binary alloy between two phases described using a classical common tangent construction. An equivalent description using the Legendre transforms of the phases is described along side which is analogous to the discussion of pure materials discussed before.

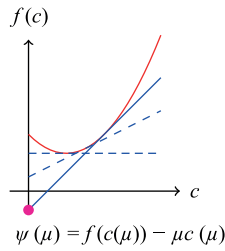


Figure 3: Schematic showing the Legendre transform of the free-energy density represented by $f(c)$ to $\Psi(\mu)$, where Ψ is the intercept and μ is the slope of the tangent to the curve at c in the curve $f(c)$.

which is the grand-canonical potential Ψ , and then plotting the **grand-potential** densities of each of the phases against the transformed variable, which is the effective diffusion potential μ . The intersection of the two curves ($\Psi^\alpha(\mu)$, $\Psi^\beta(\mu)$) occurs at the equilibrium diffusion potential μ_{eq} , which is also the slope of the common tangent at which the grand-potential densities of both phases are equal. Comparing this schematic with the case already discussed for the case of pure materials, one can analogously derive that the deviation of the diffusion potential from its equilibrium value results in a driving force for phase transition in a manner similar to the case of temperature in the case of pure materials. Noteworthy is the fact that while there is jump in internal energies between the phases at equilibrium for the case of pure materials, correspondingly, there is a jump in the compositions between the phases that exist at the same diffusion potential across an equilibrium interface.

2.3 Electrochemical interface: alloys with charged species

Consider now, the thermodynamics of an electrochemical interface. The principal difference from the thermodynamics of a purely diffusion coupled problem that was discussed for the case of a binary alloy in the preceding sections, is the fact that the constituents are now charged. This implies that diffusion of a particular species may bring about a charge localization, which must result in the generation of electrostatic potential gradients; These electrostatic potential gradients must then influence the diffusion of the different charged species in addition to the pure diffusional gradients; thereby a composite potential that is the linear superposition of the two quantities may be worked, whose gradient determines the flux of the different species. This quantity is called the electrochemical potential written as $\tilde{\mu} = \mu + zF\phi$, where z is the valence of the ion, F is the charge per

mole of electrons, ϕ is the electrostatic potential, $\tilde{\mu}$ is the electrochemical potential and μ is the diffusion potential.

As we have seen, in a classical diffusion coupled problem of phase transformation, equilibrium occurs when the compositions at the interface corresponding to the phases α and β are such that the effective diffusion potentials corresponding to each of the elements are equal in both phases, and additionally, the grand-canonical potential differences between the phases at this value of the diffusion potential is zero. Correspondingly, for the case of an electrochemical interface, equilibrium occurs when the *electrochemical potential* differences between the phases vanish. Thus, the variable analogous to the case of the diffusion potential is the effective electrochemical potential for the case of diffusion of charged species. The same can be seen from the following discussion: For a diffusion-coupled problem with no charged species, the differential change in free-energy density can be written at constant volume of the phases as,

$$df = -sdT + \mu dc, \quad (1)$$

which upon performing a Legendre transform (changing variables from c to μ) writes,

$$d(f - \mu c) = d\Psi = -sdT - cd\mu. \quad (2)$$

The variable Ψ is the grand-canonical potential density with the natural variables at constant volume as the temperature T and the diffusion potential μ , and the above expression is written with the assumption that the two phases under consideration have the same molar volumes. Difference of the grand-potential densities Ψ between the phases can be seen as a driving force for phase transition, which goes to zero at equilibrium. Also T and μ being intensive variables, at equilibrium they are the same in both phases, while the conjugate variables, s and c show a jump at the interface, with different values in each phase.

For a system with charged species, work is done when a charge $zFdc$ is transported across a potential difference ϕ , thus bringing in an additional electrostatic component to the internal energy that writes as, $zF\phi dc$ and also to the resultant change in the free-energy which thus derives,

$$df = -sdT + \mu dc + zF\phi dc. \quad (3)$$

Performing, a Legendre transform (transformation of variables from c to μ and noting that a change in dc can be accommodated in a charged system through changes in both

Grand-potential: This is Legendre transform of the Helmholtz free-energy density as also shown through the schematic in Fig. 3.

μ : $d\mu$ and electrostatic potential ϕ : $d\phi$ due to local change in charge), we derive our effective grand-potential Ψ from f in the same spirit as the previous discussion on the thermodynamics of uncharged systems as,

$$d(f - \tilde{\mu}c) = d\Psi = -sdT - cd(\mu + zF\phi) \quad (4)$$

$$= -sdT - cd\tilde{\mu}, \quad (5)$$

where the grand-canonical potential density Ψ now has its natural variable as the effective electrochemical potential $\tilde{\mu}$ and temperature T . Thus the driving force for phase transition can now be seen as a difference of the grand-potential densities $f - \tilde{\mu}c$ between the two phases, and equilibrium occurs when this difference goes to zero along with the equivalence of the effective electrochemical potential $\tilde{\mu}$ and temperature T among the two phases. Additionally, as we will see that, while the combined intensive variable i.e. $\tilde{\mu}$ is constant among the phases at equilibrium, the diffusion potential μ and electrostatic potential ϕ , both vary across the interface. This variation occurs over a finite width at the interface, that is also one of principal characteristics of the equilibrium electrochemical interface also known as the *double layer*.

2.4 Characteristics of the equilibrium electrochemical interface

In the preceding sections, we have seen the development of the thermodynamics describing the behavior of a system with charged components. In this section, we briefly understand the structure of an electrochemical interface. The rate of change of composition, in a charged electrochemical system (without a reaction), can be written as,

$$\frac{\partial c}{\partial t} = \nabla \cdot (M\nabla\tilde{\mu}), \quad (6)$$

where for simplicity we treat the mobility M as invariant of composition and phase. Since this is a problem involving charged species, localization of charges will bring about a resultant potential field. This derives from Gauss's law, and can be read as

$$\nabla(\tilde{\epsilon}\nabla\phi) = -\rho, \quad (7)$$

where ρ is the local charge density and $\tilde{\epsilon}$ is the effective permittivity, which again for simplicity we assume to be independent of composition and phase.

At equilibrium, as discussed the rate of change of composition is zero on both sides of the interface, which can only occur when $\tilde{\mu}$ is constant across both phases (for the given boundary conditions where the far-field gradients

vanish). For discussion's sake let us assume the diffusion potential of the phases to vary as,

$$\mu^\alpha = RT \ln c + B^\alpha \quad (8)$$

$$\mu^\beta = RT \ln c + B^\beta, \quad (9)$$

where B^α and B^β are constants and different from each other. Let us go deeper into the equilibration process. For this sake, let us also assume that we start from a charge neutral state where the concentration of the charged species (positive) on either side of the interface are balanced by equal and opposite ions which are immobile. Additionally, the compositions of the mobile species on both sides of the interface are assumed to be the same.

When the phases are now brought in contact, at the start, the electrostatic potentials of both phases are equal and zero as the charge density is zero. However, there is a gradient in the effective electrochemical potentials owing to difference in the diffusion potentials on both sides of the interface, which drives the flux of the ions following the direction of diffusion potential gradient. Assuming that B^α is greater than B^β would result in a flux of ions from the α to the β side, causing a depletion on the α side and accumulation on the β side, leading to a build up of positive charge on the β side and a negative charge on the α side. Further, as a consequence of the Poisson equation Eq. 7, this would result in an electrostatic potential gradient to develop opposing the flux of ions, with higher value in the β phase and lower value in the α phase. With increasing build-up of positive ions on the β side and depletion on the α side, equilibrium is reached when the flux due to the gradients in the diffusion potential $\tilde{\mu}$ exactly balances the flux due to gradients in the electrostatic potential, which is also the stage at which the gradients in the effective electrochemical potential $\tilde{\mu}$ vanishes and equilibrium is reached. From this one can calculate that the difference in potential that develops between the phases is $\Delta\phi = \frac{B^\alpha - B^\beta}{zF}$, also known as the open-circuit-potential (OCP). The variation of the electrostatic potential across the interface can be estimated by solving for the Poisson equation (Eq. 7) at equilibrium, which for one dimension writes,

$$\tilde{\epsilon} \frac{\partial^2 \phi}{\partial x^2} = -\rho(x). \quad (10)$$

In the present discussion, the charge density ρ is proportional to the departure of the composition from the starting composition c_0 as the initial state is charge neutral. Thus, the charge density writes, $\rho = zF(c - c_0)$. Additionally, at equilibrium, the effective electrochemical potential is $\tilde{\mu}_{eq}$ from

which the composition variation on each side of the interface can be related to the electrostatic potential variation as, $c = \exp\left(\frac{\tilde{\mu}_{eq} - zF\phi - B^{\alpha/\beta}}{kT}\right)$.

Thus, the preceding partial differential equation can now be written for either side of the phase interface as,

$$\tilde{\epsilon} \frac{\partial^2 \phi}{\partial x^2} \Big|_{\alpha/\beta} = -zF \left(\exp\left(\frac{\tilde{\mu}_{eq} - zF\phi - B^{\alpha/\beta}}{kT}\right) - c_o \right). \quad (11)$$

Multiplying both sides by $\frac{\partial \phi}{\partial x}$ and integrating we derive,

$$\frac{\tilde{\epsilon}}{2} \left(\frac{\partial \phi}{\partial x} \right)^2 = (c - c_o) + zFc_o (\phi - \phi_\alpha), \quad (12)$$

where as boundary conditions, one can utilize that on one side of the interface α the potential $\phi_\alpha = 0$, and on the other side, it is equal to $\Delta\phi = \frac{B^\alpha - B^\beta}{zF}$. The gradients $\frac{\partial \phi}{\partial x}$ go to zero on either phase interface while the composition c is the same as c_o on either side.

The solution to the preceding equation delivers the variation of the electrostatic potential on either side of the phase interface. While we do not venture into the complete derivation of the equations, we state here without proof that the decay length associated with the electrostatic potential, which is also known as the *Debye length* varies as $l_D \propto \frac{1}{zF} \left(\frac{\tilde{\epsilon}}{c_o} \right)^{1/2}$.

Thus, the more concentrated are the phases, with respect to the mobile species, the steeper is the variation of the electrostatic potential in the double layer. This particular region is also referred to as the diffuse layer of the Gouy-Chapman double layer.

For systems, where there is low concentration of carrier ions such as that in a semiconductor, say the phase α in the preceding example, creation of an equilibrium interface, leads to a complete depletion of carrier ions on one side of the interface. Given that there are immobile ions on either side of the interface, this leads to a region of constant charge density in the depleted region. This region has very low resistivity and is also called the *space charge*.

One of the properties of such an electrochemical interface is the asymmetry with respect to the flow of charges across the interface. When a current is imposed in a direction that reinforces the electrostatic potential, the corresponding gradient in the diffusion potential

balancing this increases, leading to a greater depletion of ions on the α side of the interface. Therefore in this direction, there is a greater resistance to the flow of current. Conversely, for the case where the imposed current reinforces the gradients of the diffusion potential, it leads to a lesser depletion and thereby lesser resistivity to the flow of ions. This asymmetric nature of the interface is normally, recorded in the (current-voltage) I-V characteristics of an electrochemical interface.

3 Basics of Phase-Field Formulations in Literature for Electrochemical Systems

In the preceding section, we have had a brief overview about the thermodynamics of electrochemical systems. In the following section, we briefly describe some of the features of phase-field models that are present in literature and their areas of application. This process is made simple by characterizing the main areas of focus in the different phase-field formulations.

3.1 The complete problem

The first class of phase-field models treat the entire electrochemical problem by solving the entire set of Poisson-Nernst-Planck equations (PNP). Ideally, in a phase-field model describing this type of phenomenon a free-energy functional is created with an contribution coming from the electrostatic energy that writes as $zFc\phi$ along with the bulk chemical thermodynamics of the phases. The order-parameter ξ differentiating the phases is utilized to create the functional, with properties contributing to the gradient energy and excess energy at the interface. The evolution of the order parameters, thereafter, follows standard dynamics ensuring minimization of free-energy. Coupled to this there are equations of mass transport, where the complete (PNP) set is written as,

$$\frac{\partial c_i}{\partial t} = \nabla \cdot \left(M(c, \xi) \nabla \left(\frac{\delta f_{chem}(c, \xi)}{\delta c_i} + z_i F \phi \right) \right) \quad (13)$$

$$\nabla \cdot (\tilde{\epsilon}(\xi) \nabla \phi) = -\rho = -\sum_i z_i F c_i, \quad (14)$$

where the first equation represents the rate of change of composition of the component i , whereby the flux of ions is determined by the gradients in the *effective electrochemical potential* $\tilde{\mu}_i = \frac{\delta f_{chem}(c, \xi)}{\delta c_i} + z_i F \phi$, z_i is the valence of the ion and f_{chem} being the chemical free-energy density, and the operator $\frac{\delta}{\delta c_i}$ represents the variational derivation w.r.t to the variable c_i . The second equation in the preceding set is the Poisson equation which allows the determination of the electrostatic potential. Notice, all properties

$\tilde{\epsilon}$, $M(c, \xi)$ are now functions of both the order-parameter and the local composition c_i .

The two equations are solved along with the evolution of the order parameter ξ at every time-step to completely solve the electrochemical problem. As is common in a electrochemical system, reactions occur, leading to the production and destruction of ions. This would need to be accounted for, in the mass-balance relations for the ions, thereby for such systems, the modified rate evolution reaction writes as,

$$\frac{\partial c_i}{\partial t} = \nabla \cdot \left(M(c, \xi) \nabla \left(\frac{\delta f_{chem}(c, \xi)}{\delta c_i} + z_i F \phi \right) \right) + \dot{R}_i, \quad (15)$$

where the \dot{R}_i represents the rate of production as a result of all the reactions in the systems. These reactions can again be classified as heterogeneous and homogeneous reactions. Heterogeneous reactions occur when components from the substrate and the electrolyte react at their interface, to form a product that either becomes a part of the substrate (deposition) or a part of the solution (dissolution). These reaction rates can be determined following the *Butler-Volmer-kinetics*. The rate of the reaction following the *Butler-Volmer* theory depends on the difference between the sum of the electrochemical potentials of the reactants and products from their equilibrium value. This departure can in turn be related to a fundamental variable in electrochemistry, which is the *overpotential*. Homogeneous reactions occur in the bulk of either the substrate or the electrolyte and their rates are determined by *laws of mass action*, which require the knowledge of the thermodynamic reaction constants.

While this way of solving the complete problem accurately describes the complete electrochemical phenomenon, a natural problem that arises when simulating morphological evolution of microstructures in the scales of microns is the wide variation of length scales. This is because, the scale of the double layer described by the Debye length extends over a few nanometers, while the effective microstructures are more than three-orders of magnitude different in size. Therefore, the complete problem of simulating a statistically relevant microstructural size, at present appears impossible. To get around this, one of the possible solutions, to this problem is to assume that there is scale separation between the properties at the scale of the electrochemical interface and the microstructural evolution. We elaborate on this in the following section.

3.2 Condition of charge neutrality

One of the ways to avoid resolving the *double layer* in the electrochemical reactions is to assume that the charges relax very fast, in comparison to the reactions that occur at the interface, whereby there is no charge localization in the time scales in where one investigates microstructural evolution. Imposing this condition implies that the electrostatic potential at any given point will be such that the total flux of charge due to the diffusional currents as well as the electrostatic potential gradients exactly cancel. This condition can be written as $\nabla \cdot i = 0$, where i is the local current. This equation delivers the electrostatic potential which is then used to solve for the local update of the different components using the preceding mass transport equations. Since there is no effective charge localization and thereby no formation of double layer, the scale of the simulations can be increased. This is useful for simulating conditions of electrodeposition, charge transfer reactions in oxide salts etc. However, certain other situations such as morphological instabilities that are inherently linked to the nature of the electrochemical interface, such as that found during the formation of macro-pores in semiconductors, where the structure of the *space charge* region is important to the resolution of the instability, the complete electrochemical problem must be resolved. This is the recent challenge in the phase-field community, which is to resolve the inherently multi-scale nature of electrochemical phenomenon during interfacial evolution.

3.3 Electromigration

An additional simplification of the complete problem is applicable for situations in metallic interconnects, where the motion of ions is directly a result of an imposed electronic wind. Here the imposed currents are much larger than the local electrostatic potential gradients created as a result of local charge generation, whereby the flux of ions can be directly linked to the imposed electrostatic potential density and the update of the compositions of ions can be derived. Local inhomogeneities due to difference in electronic conductivities can be resolved using the general structure of the phase-field order parameters to interpolate the conductivity properties in the entire domain and the solution to the Laplace equation, $\nabla \cdot (\tilde{\epsilon}(\xi) \nabla \phi) = 0$, delivers the electrostatic potential field, in such a system.

4 Phase-Field Models in Literature

In the previous sections, we have had an overview of the thermodynamics as well as the basis of the

different phase-field formulations for different situations in electrochemical phenomenon. In this section, we summarize the progress in the development and application of phase field models to studying electrochemical interfacial phenomenon whereby we elaborate about the different models, their structure and areas of applications. In particular, we highlight those phase field studies which aim at understanding technologically important electrochemical processes, namely, electrodeposition, electromigration and intercalation processes in battery electrode materials.

Among these, the first phase-field model discussing the solution to the complete electrochemical problems is provided by Guyer et al.^{4,5} Here, they demonstrate the formation of an interfacial double layer (similar to classical Guoy-Chapman-Stern layer) and its structural changes with current and established interrelations between the physical parameters of the electrochemical system and the phase-field parameters such as the gradient energy coefficient and kinetic coefficients. Their model uses a phase-field variable (similar to ξ) to distinguish between the electrode and the electrolyte phases. Ions are assumed to be substitutional species with equal partial molar volume while the electrons are assumed to be interstitial species with zero partial molar volume. The model draws parallels between the dynamics of an electrode-electrolyte interface and that of a solid-melt interface as is clear from the similarity in thermodynamics from the discussion in the previous sections. Since the model illustrates the solution to the complete (PNP) set, it incorporates interactions between charged species and electrostatic potential, which requires the solution of Poisson's equation Eq. 7 at every point in the system.

The electrical permittivity is assumed to be position-dependent to distinguish between the dielectric properties of electrode and electrolyte through interpolation functions created using the phase-field variable ξ . The equilibrium distribution of electrostatic potential within the electrolyte obtained from their model shows excellent agreement with the classical Guoy-Chapman and Deby-Huckel theories. The dynamic solutions to their phase-field model show the development of nonlinear current-overpotential relation. However, the numerical solutions of the governing equations were limited to one dimension since their primary objective was to develop a phase-field approach that could capture the formation of electrochemical double layer. Although their phase-field model compares

well with the classical sharp interface theories of electrochemistry and resolve the double layer accurately it is limited by the thickness of electrochemical double layer and cannot be applied to systems whose dimensions exceed a few nanometers. Therefore, the development of models to simulate the evolution of realistic microstructures (where the length scale varies between hundreds of nanometers and several microns) during electrochemical processes poses a crucial challenge both physically and numerically.¹⁹

4.1 Phase-field models of electrodeposition

Electrodeposition broadly refers to electrochemical processes, which involve reduction of dissolved metal cations to form a thin coherent coating on suitable electrode surfaces using electric current. Electrodeposition has been applied since ancient times to protect metal surfaces from corrosion and produce decorative surface finishes. In recent times, electrodeposition has been extensively used for the fabrication of advanced microelectronic devices and nanobiosystems.²⁰ To control and optimize the morphology of the electrodeposits at different length scales, it is crucial to understand the effect of electrodeposition process parameters on the morphological evolution of the electrodeposits.

Shibuta et al. adopted the model developed by Pongsaksawad et al. to simulate electrodeposition of copper from copper-sulfate solution.^{8,11} The difference here is the bulk chemical thermodynamics, which is similar to the Kim-Kim-Suzuki model of diffusional coupled phase transformation, wherein, two composition fields are used, one pertaining to the electrolyte and the other to the electrode. The composition fields satisfy the condition of equal diffusion potential in each phase as well as the condition of local mass balance, i.e the local composition is the weighted average of the composition fields in the electrode and the electrolyte with the weighting factor being an interpolation function constructed out of the phase-field parameter ξ . The driving force for phase transition is then formulated as the difference of the grand-potential densities constructed out of the composition fields in either phase. Their study is aimed at understanding the effect of copper ion concentration in electrolyte, applied voltage and interfacial anisotropy on the dendritic morphology of electrodeposited copper. Further, we should note that the model can be applied to those electrochemical processes where the influence of interfacial double layer on interface dynamics can be neglected. A similar simplified model based on

Allen-Cahn kinetics was developed by Shibuta et al. to study bridge formation and dissolution through electrochemical reactions in nanometer scale switches.²¹

Okajima et al. extended the two-dimensional phase-field model developed by Shibuta et al. by incorporating Butler-Volmer kinetics at the electrode/electrolyte interface.²² The model relates the growth velocity of the interface to the *overpotential* arising due to electrochemical redox reaction. The asymmetry in redox reactions is described by the difference in exchange current densities in the Butler-Volmer equation,

$$i = i_{\text{ox}}^0 \exp\left(\frac{\alpha Fz\eta}{RT}\right) - i_{\text{red}}^0 \exp\left(\frac{-(1-\alpha)Fz\eta}{RT}\right), \quad (16)$$

where i_{ox}^0 and i_{red}^0 are the exchange current densities of the oxidation and reduction reactions, η denotes the overpotential (difference between electrode potential during the redox event and the equilibrium electrode potential) and α is the asymmetric charge transfer coefficient. Butler-Volmer kinetics was incorporated in the model by adding an exponential term to the diffusion coefficient where the exponent is a function of overpotential η and the asymmetry parameter α . A charge conservation equation was solved to compute electrostatic potential distribution assuming local electroneutrality condition at the interface. Their simulations of dendritic growth of electrodeposits show asymmetry in growth velocity as function of overpotential in accordance with Butler-Volmer kinetics. Shibuta and coworkers applied their model to study dendritic growth of electrodeposited uranium and zirconium from molten salt and estimated the threshold concentration of cations in the molten salt as a function of current density for transition of the growth front from planar to dendritic.^{23,24}

Liang et al. proposed a nonlinear phase-field model to study electrode/electrolyte interface evolution during electrochemical reactions where the thermodynamic driving force was modified to reproduce Butler-Volmer kinetics.²⁵ They modified the Allen-Cahn equation to describe a nonlinear relation between the rate of phase transformation and the thermodynamic driving force following the principles of rate theory of chemical reaction kinetics. The nonlinear model reproduces Butler-Volmer kinetics as a function of overpotential in the sharp interface limit. Liang and Chen extended the nonlinear phase-field formalism to model lithium electrodeposition on electrode surface during charging operation of a lithium-ion battery.^{26–28} In addition to the nonlinear phase-field equation describing motion of electrode-electrolyte

interface, they solve an ambipolar diffusion equation for Li^+ cations assuming local charge neutrality condition within the electrolyte and an electrostatic Poisson's equation which includes a reaction current term describing the asymmetry in the generation and depletion of charge at the electrode-electrolyte interface. The model predicts the formation and growth of dendritic morphology of Li-electrodeposits as function of charge rate and qualitatively investigates the role of varying current density and rate constants on the morphology of electrodeposits.

Ely et al. reported a phase-field model describing the growth and coarsening of heterogeneously nucleated electrodeposits of lithium.²⁹ The total free energy of the electrolyte-dendrite system is described using a variational framework and includes bulk driving force for electrochemical reduction of lithium ions, electrolyte-electrodeposit interfacial energy, and the work of adhesion due to wetting of the substrate by electrodeposited lithium. The temporal evolution of the solid phase is governed by a modified Allen-Cahn equation where the driving force includes a non-zero interfacial reaction rate derived using nonlinear Butler-Volmer kinetics in accordance with the nonlinear model proposed by Liang et al.²⁵ Charge density is treated as a locally conserved order parameter and its evolution is described using Cahn-Hilliard equation. The phase field simulations with different degrees of wetting show an increase in curvature-induced electro-dissolution with increase in contact angle, albeit that the dendritic tip velocity remains the same for all wetting conditions.

Recently Cogswell developed an electrochemical potential based phase-field model to study dendritic growth during electrodeposition of metals incorporating Marcus kinetics for concentrated solutions where the reactants and products do not change their atomic structure during electron transfer process.³⁰ The asymmetric transfer coefficient in the Butler-Volmer current-overpotential equation (Eq. 16) is defined using Marcus theory of electron transfer. Local electroneutrality condition is imposed to derive a current conservation equation. The model was parametrized using a dimensionless Damkohler number $Da = \frac{i_0 V_m / nF}{D/L}$, where n is the number of electrons transferred, D is the ionic diffusivity and L is the separation distance between two electrodes. The model was used to simulate the effect of electrolyte concentration and electrochemical reaction kinetics on dendritic growth of electrodeposited zinc. The formulation of this model can be seen as a thermodynamic

re-formulation of the model of Shibuta et al., with the use of the diffusion potential μ as the state variable instead of the different composition fields akin to the KKS¹⁰ type of formulations. This re-formulation can be seen in similar lines following^{31,32} which were performed for the case of pure diffusion coupled problems.

We note that the afore-mentioned phase field models describing morphological evolution during electrodeposition assume negligible interface resistance and impose local electroneutrality condition although these assumptions are strictly valid when the structure of electrical double layer does not affect electrochemical interface kinetics. In other words, when morphological evolution is diffusion-controlled rather than charge-transfer limited, solution of charge conservation equation may suffice.¹⁹

4.2 Phase-field models on Li-ion intercalation in batteries

Electrochemical phase-field models also find their application in the study of intercalation dynamics (insertion and extraction of ions in cathode and anode materials) in batteries. Of particular interest are mesoscale models for intercalation of Li-ions in cathode nanoparticles and the subsequent phase transformations within the intercalating particles. A typical cathode of a Li-ion battery contains carbon coated intercalating particles packed in a porous composite structure. A fundamental understanding of Li-ion intercalation dynamics during charging/discharging is crucial for optimization of battery performance.³³

Transition metal based phospho-olivine type compounds $LiMPO_4$ ($M = Fe, Mn, Co, Ni$) have emerged as candidates for intercalating cathode materials in Li-ion batteries due to their high storage capacity, high discharge rate and optimum operating voltage.^{33–35} Li_xFePO_4 olivine exhibits a miscibility gap at room temperature and forms an equilibrium mixture of Li-poor $Li_{0.032}FePO_4$ and Li-rich $Li_{0.962}FePO_4$ phases.³⁶ The propensity of phase-separation in Li_xFePO_4 can be altered with change in the intercalating particle morphology, application of electric overpotential, doping bulk electrode with transition metal ions and applying conductive coating on particles (see^{37,38} for detailed reviews and references therein). In-situ experiments, first-principles calculations and atomistic simulations show strongly anisotropic one-dimensional diffusion of lithium in bulk olivine structure.^{39–41} Moreover, first-principles calculations of elastic properties reveal strong anisotropy in elastic constants (elastic stiffness tensor shows orthorhombic symmetry), composition-

dependence of elastic moduli, and anisotropy in misfit strains.^{42,43} Therefore, to understand the role of anisotropy in the parameters affecting electrochemically induced phase transformations within intercalated Li_xMPO_4 particles, there have been efforts to develop mesoscale phase-field models of morphological evolution during the intercalation process.^{14–16,37,44–49}

The first attempt in phase-field modeling of intercalation process is by Han et al. who implemented a phase field model in one dimension to investigate the diffusion of Li ions and the diffusional phase transformations inside the olivine particles during intercalation.⁴⁴ They compared the effective chemical diffusion coefficients obtained from the phase-field simulations with those obtained experimentally using PITT (Potentiostatic Intermittent Titration Technique) and GITT (Galvanostatic Intermittent Titration Technique).

In a later study, Singh et al. developed a phase field model where they incorporated anisotropic ionic mobility in the olivine structure and surface reactions governing the flux of Li-ions across the electrolyte/electrode interface.¹⁴ Tang et al. developed a phase field model to study the effect of size, overpotential and strain energy on the phase transition pathways in nanoscale phospho-olivines. They used their model to study the competition between crystalline to amorphous transition and phase separation between the Li-rich and Li-poor phases in nanoscale olivines.^{37,46} Bai et al. studied the effect of overpotential on the suppression of phase-separation in intercalating cathode particles during battery discharge using an electrochemical phase-field model.¹⁵ However, all of these studies were restricted to one-dimension or simplified two-dimensional geometries and neglected the effect of coherency strain.

Cogswell and Bazant included elastic stress effects arising due to anisotropic misfit strain between Li-rich and Li-poor phases to study the morphology of intercalation in single Li_xFePO_4 nanoparticles where x lies within the spinodal limit.¹⁶ Their two-dimensional simulations show the formation of striped morphology of lithiated and de-lithiated phases. They also observed that coherency strains can modify the solubility limit of lithium and may lead to suppression of phase separation with varying particle size and magnitude of misfit strain. Bazant developed a phase-field theory of chemical kinetics and charge transfer based on the principles of non-equilibrium thermodynamics and created a modified “Allen-Cahn-Reaction” model coupled with Cahn-Hilliard equation of mass transport to study

the dynamics of electrochemically induced phase transformations within nanoparticles.⁴⁷ Welland et al. implemented a three-dimensional multi-physics phase-field model that incorporates anisotropic, concentration dependent moduli, misfit strain and anisotropic surface wetting to study phase separation in phospho-olivine nanoparticles as a function of lithium concentration.⁴⁸ They observe that the stability of phases crucially depends on their surface wetting characteristics. Further, they report disappearance of miscibility gap when the intercalating particle sizes fall below five nanometers. However, the effect of Butler-Volmer boundary condition on the surface of the particle on the phase transformation pathways is not evident in their model. Recently, Hong et al. implemented a phase-field model based on spectral smoothed boundary method to study lithium intercalation in a Li_xFePO_4 nanoparticle immersed in lithium-ion rich electrolyte.⁴⁹ Heterogeneous nucleation of Li-rich and Li-poor phases on particle surface as well as flux of lithium atoms, through a charge transfer process across particle surface (Butler-Volmer boundary condition), are taken into account. Their simulations in two dimension show growth of Li-rich plates along elastically soft directions. Although the phase-field models do capture some essential morphological features during intercalation, we should note that the simulations are restricted to a single intercalating particle while nanoscale state-of-charge mapping of intercalation pathway in many-particle electrode show the formation of a majority of completely lithiated or delithiated particles during discharging of battery.⁵⁰ Moreover, *in-situ* visualization of lithium transport and intercalation in model FeF_2 nanoparticles using nanoscale imaging suggest new pathways of Li-ion transport and subsequent phase transformations during intercalation.⁵¹ Thus, we need to develop quantitative phase-field models where crucial thermodynamic parameters such as gradient energy coefficient and interfacial length scale can be ascertained from *ab initio* calculations to accurately describe chemical segregation and surface effects on electrochemically induced phase transformations.⁵² Such quantitative models need to be extended to multi-particle electrodes to understand the development of intercalation morphology during charging-discharging cycles of batteries.

4.3 Other applications of electrochemical phase-field models

Pongsaksawad et al. developed a phase-field model to study electrochemical interface evolution during transport-limited electrolytic

steel refining and smelting processes.^{11,19,53} The model was applied to investigate topological evolution of cathode surface in two- and three-dimensions during mass transport limited electrolysis with fast redistribution of charge. Thus, the electrostatic potential can be retrieved through the condition of *electroneutrality*, which makes it applicable to situations when electrochemical reactions are “mass-transport-limited”, i.e. the changes at the scale of the electrochemical interface occur much faster compared to the rate of the reactions as well as microstructural evolution. Additionally, they coupled the Navier-Stokes equation to their phase-field model to account for convective flow in liquid electrolytic systems.

Gathright et al. apply the model developed by Guyer et al.⁴⁵ to study the development of Nernst electromotive force in a solid-electrolyte gas sensor containing chemically active species.¹⁷ The model does not consider morphological changes and solves Poisson’s equation for electrostatic equilibrium to fully resolve the Debye layer for a prescribed interface morphology. The model is implemented to simulate electrochemical impedance spectra for generic electrode-electrolyte systems which compare well with experimental data.^{54,55} However, the simulations are restricted to small length scales to ensure accurate numerical discretization of the Debye layer.

Electromigration is described as electric field induced flow of matter resulting from momentum transfer between conduction electrons and charged ions, and is a crucial factor determining the reliability of solder interconnects in integrated circuits.⁵⁶ There are several phase field models reported in literature that examine the influence of external electric field on the electromigration and coalescence of microvoids in solder interconnects.⁵⁷⁻⁶¹ These models particularly investigate the interactions between surface diffusion of charged ions and electromigration induced mass flux.

5 Conclusions

In this review, we have presented an overview of the thermodynamics of electrochemical systems and related it to the thermodynamics of pure materials and alloys. Here we elaborate on the characteristics of the electrochemical interface and the additional length scale of the Debye-layer which differentiates it from the equilibrium interfaces of pure materials and alloys. Thereafter, we give a brief overview of the basis of phase-field models proposed for describing electrochemical phenomena, followed by a brief discussion of the work in literature related to each

of the applications of phase-field models. While this review presents the state-of-the art phase-field models in the community, it also clarifies at various places the several modeling and numerical challenges for describing electrochemical reactions using phase-field models owing to the multi-scale nature of the problem. This is the motivation for future work in the formulation of better models and numerical techniques.

Received 16 August 2016.

References

1. L. Chen, *Annual Review in Materials Research* **32**, 113 (2002).
2. I. Steinbach, *Modeling and Simulation in Mat. Sci. and Engg* **17**, 073001 (2009).
3. B. Nestler and A. Choudhury, *Current Opinion in Solid State and Materials Science* **15**, 93 (2011).
4. J.E. Guyer, W.J. Boettinger, J.A. Warren and G.B. McFadden, *Physical Review E* **69**, 021603 (2004).
5. J.E. Guyer, W.J. Boettinger, J.A. Warren and G.B. McFadden, *Physical Review E* **69**, 021604 (2004).
6. S. Chakraborty, *Physical Review Letters* **101**, 184501 (2008).
7. Y. Shibuta, Y. Okajima and T. Suzuki, *Scripta Materialia* **55**, 1095 (2006).
8. Y. Shibuta, Y. Okajima and T. Suzuki, *Science and Technology of Adv. Mat.* **8**, 511 (2007).
9. M.S. Park, S.L. Gibbons and R. Arróyave, *Acta Materialia* **61**, 7142 (2013).
10. S.G. Kim, W.T. Kim and T. Suzuki, *Phys. Rev. E* **58**, 3316 (1998).
11. W. Pongsaksawad, A.C.P. IV and D. Dussault, *Journal of the Electrochemical Society* **154**, F122 (2007).
12. H. Assadi, *Modeling and Simulation in Materials Science and Engineering* **14**, 963 (2006).
13. T.R. Ferguson and M.Z. Bazant, *Journal of the Electrochemical Society* **159**, A1967 (2012).
14. G.K. Singh, G. Ceder and M.Z. Bazant, *Electrochimica Acta* **53**, 7599 (2008).
15. P. Bai, D.A. Cogswell and M.Z. Bazant, *Nano Letters* **11**, 4890 (2011).
16. D.A. Cogswell and M.Z. Bazant, *ACS Nano* **6**, 2215 (2012).
17. W. Gathright, M. Jensen and D. Lewis, *Electrochemistry Communications* **13**, 520 (2011).
18. M.-O. Bernard, M. Plapp and J.F. Gouyet, *Physical Review E* **68**, 011604 (2003).
19. A.C. Powell IV, Y. Shibuta, J.E. Guyer and C.A. Becker, *JOM* **59**, 35 (2007), ISSN 1047-4838.
20. W. Schwarzacher, *Interface* **15**, 32 (2006).
21. Y. Shibuta, Y. Okajima and T. Suzuki, *Scripta Materialia* **55**, 1095 (2006), ISSN 1359-6462.
22. Y. Okajima, Y. Shibuta and T. Suzuki, *Computational Materials Science* **50**, 118 (2010), ISSN 0927-0256.
23. Y. Shibuta, T. Sato, T. Suzuki, H. Ohta and M. Kurata, *Journal of Nuclear Materials* **436**, 61 (2013), ISSN 0022-3115.
24. Y. Shibuta, S. Unoura, T. Sato, H. Shibata, M. Kurata and T. Suzuki, *Journal of Nuclear Materials* **414**, 114 (2011), ISSN 0022-3115.
25. L. Liang, Y. Qi, F. Xue, S. Bhattacharya, S.J. Harris and L.-Q. Chen, *Physical Review E* **86**, 051609 (2012).
26. L. Liang and L.-Q. Chen, *Applied Physics Letters* **105**, 263903 (2014), ISSN 0003-6951.
27. H.-W. Zhang, Z. Liu, L. Liang, L. Chen, Y. Qi, S.J. Harris, P. Lu and L.-Q. Chen, *ECS Transactions* **61**, 1 (2014), ISSN 1938-6737.
28. L. Chen, H.W. Zhang, L.Y. Liang, Z. Liu, Y. Qi, P. Lu, J. Chen and L.-Q. Chen, *Journal of Power Sources* **300**, 376 (2015), ISSN 0378-7753.
29. D.R. Ely, A. Jana and R.E. García, *Journal of Power Sources* **272**, 581 (2014), ISSN 0378-7753.
30. D.A. Cogswell, *Physical Review E* **92**, 011301 (2015).
31. A. Choudhury and B. Nestler, *Phys. Rev. E* **85**, 021602 (2011).
32. M. Plapp, *Phys. Rev. E* **84**, 031601 (2011).
33. Y.-M. Chiang, *Science* **330**, 1485 (2010), ISSN 0036-8075.
34. M. Wagemaker and F.M. Mulder, *Accounts of Chemical Research* **46**, 1206 (2012), ISSN 0001-4842.
35. K. Kang, Y.S. Meng, J. Bréger, C.P. Grey and G. Ceder, *Science* **311**, 977 (2006), ISSN 0036-8075.
36. A. Yamada, H. Koizumi, S.-I. Nishimura, N. Sonoyama, R. Kanno, M. Yonemura, T. Nakamura and Y. Kobayashi, *Nature Materials* **5**, 357 (2006), ISSN 1476-1122.
37. M. Tang, W.C. Carter and Y.-M. Chiang, *Annual Review of Materials Research* **40**, 501 (2010), ISSN 1531-7331.
38. P. Bai and G. Tian, *Electrochimica Acta* **89**, 644 (2013), ISSN 0013-4686.
39. D. Morgan, A. Van der Ven and G. Ceder, *Electrochemical and Solid-State Letters* **7**, A30 (2004), ISSN 1099-0062.
40. S.-I. Nishimura, G. Kobayashi, K. Ohoyama, R. Kanno, M. Yashima and A. Yamada, *Nature Materials* **7**, 707 (2008), ISSN 1476-1122.
41. R. Malik, D. Burch, M. Bazant and G. Ceder, *Nano Letters* **10**, 4123 (2010), ISSN 1530-6984.
42. T. Maxisch and G. Ceder, *Physical Review B* **73**, 174112 (2006).
43. R. Deshpande, Y. Qi and Y.-T. Cheng, *Journal of the Electrochemical Society* **157**, A967 (2010), ISSN 0013-4651.
44. B. Han, A. Van der Ven, D. Morgan and G. Ceder, *Electrochimica Acta* **49**, 4691 (2004), ISSN 0013-4686.
45. D. Burch and M.Z. Bazant, *Nano Letters* **9**, 3795 (2009), ISSN 1530-6984.
46. M. Tang, H.-Y. Huang, N. Meethong, Y.-H. Kao, W.C. Carter and Y.-M. Chiang, *Chemistry of Materials* **21**, 1557 (2009), ISSN 0897-4756.
47. M.Z. Bazant, *Accounts of Chemical Research* **46**, 1144 (2013), ISSN 0001-4842.

48. M.J. Welland, D. Karpeyev, D.T. O'Connor and O. Heinonen, *ACS Nano* **9**, 9757 (2015), ISSN 1936-0851.
49. L. Hong, L. Liang, S. Bhattacharyya, W. Xing and L.-Q. Chen, *Physical Chemistry Chemical Physics* **18**, 9537 (2016).
50. W.C. Chueh, F. El Gabaly, J.D. Sugar, N.C. Bartelt, A.H. McDaniel, K.R. Fenton, K.R. Zavadil, T. Tyliczszak, W. Lai and K.F. McCarty, *Nano Letters* **13**, 866 (2013), ISSN 1530-6984.
51. F. Wang, H.-C. Yu, M.-H. Chen, L. Wu, N. Pereira, K. Thornton, A. Van der Ven, Y. Zhu, G.G. Amatucci and J. Graetz, *Nature Communications* **3**, 1201 (2012).
52. M.E. Stournara, R. Kumar, Y. Qi and B.W. Sheldon, *Physical Review E* **94**, 012802 (2016).
53. W. Pongsaksawad, *Numerical Modeling of Interface Dynamics and Transport Phenomena in Transport-Limited Electrolysis Processes*, Ph.D. thesis, Massachusetts Institute of Technology (2006).
54. W. Gathright, M. Jensen and D. Lewis, *Journal of Materials Science* **47**, 1677 (2012), ISSN 0022-2461.
55. W. Gathright, M. Jensen and D. Lewis, *ECS Transactions* **35**, 1077 (2011), ISSN 1938-6737.
56. D. Pierce and P. Brusius, *Microelectronics Reliability* **37**, 1053 (1997).
57. M. Mahadevan and R.M. Bradley, *Physica D: Nonlinear Phenomena* **126**, 201 (1999).
58. J.W. Barrett, R. Nürnberg and V. Styles, *SIAM Journal on Numerical Analysis* **42**, 738 (2004).
59. D.N. Bhate, A. Kumar and A.F. Bower, *Journal of Applied Physics* **87**, 1712 (2000).
60. M.S. Park, S. Gibbons and R. Arróyave, *Acta Materialia* **61**, 7142 (2013).
61. S.-B. Liang, C.-B. Ke, M.-B. Zhou and X.-P. Zhang, in *Electronic Packaging Technology (ICEPT), 2015 16th International Conference on (IEEE, 2015)* pp. 260–265.



Saswata Bhattacharyya is an Assistant Professor in the Department of Materials Science and Metallurgical Engineering in Indian Institute of Technology Hyderabad. He obtained his PhD from Indian Institute of Science for his thesis on “Evolution of multivariant microstructures with anisotropic misfit: A phase-field study” under the supervision of Prof. T. A. Abinandanan and carried out his postdoctoral research on the development of phase-field models of microstructural evolution in alloys and oxides with Prof. Long-Qing Chen at The Pennsylvania State University. His research interests include phase-field modeling of microstructural evolution in alloys and oxides and phase transformations in electronic and energy storage materials. He has authored and coauthored around twenty-five technical papers on the development and implementation of phase-field models to study phase transformations in materials.



Soumya Bandyopadhyay is currently a Graduate Student in the Department of Materials Science and Metallurgical Engineering in Indian Institute of Technology Hyderabad. His research involves phase field modeling of domain dynamics in multiferroic systems and dielectric degradation due to charge transport.



Abhik Choudhury is an Assistant Professor in the Department of Materials Engineering at the Indian Institute of Science, Bangalore since Nov. 2013. He has graduated from the Indian Institute of Technology with a dual degree in 2008 from the department of metallurgical and materials engineering, with a major in Materials Engineering and a minor in theoretical computer science. Thereafter he received his PhD from the University of Karlsruhe (Germany) under the supervision of Prof. Dr. Britta Nestler on “Quantitative phase-field modeling of multi-component diffusion coupled phase transformations” which concluded in 2012. He continued as a Post-doctoral researcher with Prof. Dr. Mathis Plapp at the Ecole Polytechnique Paris, where he worked on developing a phase-field model for understanding morphological instabilities originating during electrochemical reactions, and subsequently joined the Indian Institute of Science as a faculty in 2013. His research interests include studies on pattern formation during phase transformations such as solidification, electrochemical reactions and stress mediated evolution of microstructures.